THERMAL STUDY OF A 2 KELVIN COPPER PHOTOCATHODE IN A CW SRF GUN CAVITY *

D. Bazyl†, K. Flöttmann, E. Vogel, I. Zagorodnov
Deutsches Elektronen-Synchrotron DESY, Hamburg, Germany

Abstract

We assess the thermal behavior of a cryogenically cooled copper photocathode integrated into a continuous-wave superconducting radio-frequency injector cavity through direct thermal contact. A coupled three-dimensional thermal-electromagnetic model incorporating both the bulk photocathode and the injector cavity is presented. For the current injector design, the laser heat load is predicted to have a negligible effect on the intrinsic quality factor of the cavity. The cryogenic stability of the copper cathode is identified as the primary operational constraint. To address the associated cooling challenges, we propose a modified cathode plug geometry.

INTRODUCTION

A superconducting radio-frequency (SRF) photoinjector is under development at DESY for continuous wave (CW) operation in a future upgrade of the European X-ray Free-Electron Laser [1, 2]. The cathode is threaded onto the rear wall of the superconducting niobium cavity [3] (Fig. 1, left), an injector design that has reached 50 MV/m in vertical tests [4]. For 100 pC bunches at 1 MHz with a target QE of $(1\text{–}2.5) \times 10^{-4}$ at 257 nm, the required average UV laser power is 2–5 W (Fig. 1, right), comparable to the ~1 W RF dissipation on the cavity rear wall at 50 MV/m. This laser heat load must be assessed for both thermal stability and potential quality factor degradation. We invistigate the thermal problem using COMSOL MULTIPHYSICS® v6.3 [5]. A more detailed description including a two-temperature model for the emitting surface is given in [6].

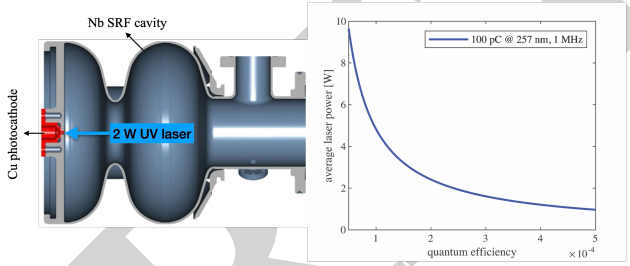

Figure 1: Left: 3D layout of the CW SRF injector cavity with integrated copper photocathode. Right: average laser power required for a Cu photocathode as a function of QE, assuming 1 MHz repetition rate and 100 pC bunch charge (257 nm excitation).

* Work performed in the framework of R&D for future accelerator operation modes at the European XFEL and financed by the European XFEL GmbH.
† dmitry.bazyl@desy.de

THERMAL-ELECTROMAGNETIC MODEL

The laser heat load is applied as a time-averaged inward heat flux boundary condition on the cathode emission surface:

$$-\mathbf{n} \cdot (k\nabla T) = q_{\text{avg}}, \quad q_{\text{avg}} = P_{\text{avg}}(1-R)/A_{\text{spot}}, \tag{1}$$

where P_{avg} is the incident laser power, $R = 0.36$ is the copper reflectivity at 257 nm, and $A_{\text{spot}} = \pi r_{\text{spot}}^2$ is the laser spot area with $r_{\text{spot}} = 430\,\mu\text{m}$. This steady-state approach was validated against a full transient simulation with periodic 1 MHz pulsed heating. At the Cu–In–Nb contact point, the transient solution stabilizes to a mean temperature matching the steady-state result, confirming that the bulk cathode responds to the average power input [6].

The computational model (Fig. 2, left) consists of the copper photocathode plug, the niobium cavity back wall, and the RF vacuum volume. A 1/8th section is simulated due to partial axial symmetry of the back wall. Temperature-dependent thermal conductivities for copper (RRR = 300) [7] and niobium (RRR = 300) [8] are used.

The primary heat transfer path from the cathode to the niobium is the Cu–In–Nb contact, characterized by a thermal contact resistance R_{tc}. Since specific data for this joint are not available, we adopt a conservative estimate $R_{tc} \approx 1.0 \times 10^{-3}\,\text{K}\,\text{m}^2/\text{W}$ at 2 K, extrapolated from measurements on similar Nb–In–Al joints [9] using the T^{-3} scaling consistent with phonon-dominated interfacial transport. This resistance is applied as a boundary condition imposing a temperature discontinuity proportional to the normal heat flux across the interface.

The cooling at the Cu–He II and Nb–He II interfaces is governed by the Kapitza conductance $h_K = aT^3$ [10], with a clean copper surface ($a = 1.0 \times 10^3\,\text{W}\,\text{m}^{-2}\,\text{K}^{-4}$) and BCP cavity-grade niobium ($a = 4.0 \times 10^2\,\text{W}\,\text{m}^{-2}\,\text{K}^{-4}$). The helium bath temperature is $T_{\text{bath}} = 2\,\text{K}$.

The electromagnetic coupling is implemented through a surface impedance boundary condition on the cavity back wall with $Z_s(T) = R_s(T) + iX_s$. The BCS surface resistance at 1.3 GHz is given by:

$$R_s(T) = R_{\text{res}} + \frac{C}{T} f^2 \exp\left(-\frac{\Delta(T)}{k_B T}\right), \tag{2}$$

where the free parameters $R_{\text{res}} = 8.3\,\text{n}\Omega$ and $C = 31182\,\text{n}\Omega\cdot\text{K/GHz}^2$ were fitted to measurements of the DESY 16G09 cavity.

RESULTS

The analysis of the baseline cathode geometry reveals a potential cooling limitation. For a nominal incident laser

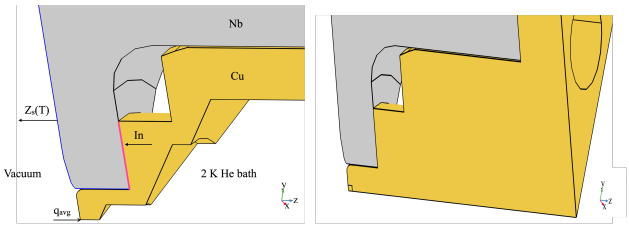

Figure 2: Left: schematic of the computational domains and principal boundary conditions at the Cu–Nb interface. Right: improved copper cathode plug geometry.

power of 2 W, the steady-state solution predicts that the temperature on the helium-wetted copper surface exceeds the helium saturation temperature ($T_{sat} \approx 2.0$ K at ~ 31 mbar) by $\Delta T \approx 0.4$ K, indicating a localized hot spot on a conical protrusion (Fig. 3, left). The thermal performance is constrained by a conductive bottleneck: the narrow cross-section of the protrusion creates a significant internal thermal impedance that concentrates the heat flux before it can be distributed across the wetted interface. An improved cathode plug geometry (Fig. 2, right) increases the local cross-section in the vicinity of the hot spot, providing a lower impedance path for lateral heat conduction. For this geometry at $P_{avg} = 2$ W, the peak temperature is $T_{peak} \approx 2.07$ K ($\Delta T \approx 0.07$ K), as shown in Fig. 3 (right). At $P_{avg} = 5$ W, the peak reaches $T_{peak} \approx 2.14$ K. To check for thermal-RF feedback runaway,

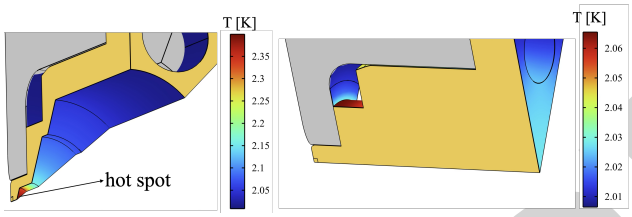

Figure 3: Steady-state temperature on the helium-wetted surfaces of the copper plug and adjacent niobium back wall for $P_{avg} = 2$ W. Left: baseline geometry. Right: improved geometry.

the coupled thermal-electromagnetic model was solved iteratively. The calculated RF losses were added back into the thermal model as a heat source and the loop was repeated. At $P_{avg} = 5$ W, the iterative scheme converges after the second iteration (Fig. 4, left). The total RF power dissipated at the back wall increases by only 2.8% relative to the isothermal ($T = 2$ K) case. The area of maximum temperature increase is small and coincides with the region of low magnetic field of the TM_{010} mode, rendering the effect of localized heating on the integrated RF power dissipation negligible. A sensitivity study varying R_{tc} from zero to a factor of two confirms that uncertainties in the Cu–In–Nb contact resistance have only a minor impact on both the copper temperature (spread < 6 mK) and the total dissipated RF power (variation well below 1%).

CONCLUSION

The analysis identified a potential cryogenic instability in the baseline cathode geometry, where even at the nominal laser power (2 W) the helium-wetted Cu interface is predicted to exceed the helium saturation temperature by about 0.4 K. The improved plug geometry maintains the interface temperature near saturation ($\Delta T \approx 0.07$ K) at 2 W. Assuming cryogenic stability is established, we confirm that the SRF injector remains electromagnetically stable: the thermal-RF feedback loop converges rapidly. The primary thermal consideration for the injector design is therefore the management of the direct cryogenic cooling at the cathode rather than RF-thermal feedback effects. Operation at higher laser loads will benefit from further dedicated cryogenic analysis and geometry optimization.

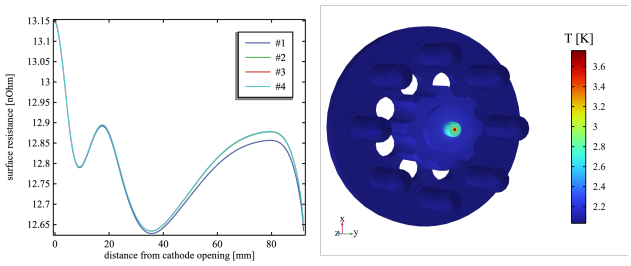

Figure 4: Left: surface resistance profiles along the Nb back wall for four iterations of the coupled model at $P_{avg} = 5$ W. Right: steady-state temperature distribution in the Cu plug (4th iteration, $P_{avg} = 5$ W).

ACKNOWLEDGMENTS

Authors thank H. Weise for reading this manuscript and providing valuable comments. We thank D. Reschke for providing experimental data on surface resistance and thermal conductivity for the injector cavity, as well as for reading the manuscript and providing valuable comments. We thank A.K. Dhillon for providing critical comments on the cryogenic operating conditions of the SRF injector and the associated helium-II heat-transfer physics. We thank M. Wenskat for fruitful discussions on questions of the cryogenic stability in SRF environment. Authors thank W. Decking and H. Weise for their interest and support of this work. We thank H. Sinn, M. S. Tavakkoly and F. Yang (European XFEL GmbH) for useful discussion on ultra-fast laser heating. We thank support team of Comsol Multiphysics GmbH for assistance on technical questions.

REFERENCES

[1] W. Decking *et al.*, "A MHz-repetition-rate hard X-ray free-electron laser driven by a superconducting linear accelerator", *Nat. Photonics*, vol. 14, no. 6, pp. 391–397, 2020. doi:10.1038/s41566-020-0607-z

[2] R. Brinkmann, E. A. Schneidmiller, J. Sekutowicz, and M. V. Yurkov, "Prospects for CW and LP operation of the European XFEL in hard X-ray regime", *Nucl. Instrum. Methods Phys. Res. A*, vol. 768, pp. 20–25, 2014. doi:10.1016/j.nima.2014.09.039

[3] E. Vogel *et al.*, "SRF Gun Development at DESY", in *Proc. LINAC'18*, Beijing, China, pp. 105–108, Jan. 2019. doi:10.18429/JACoW-LINAC2018-MOPO037

[4] E. Vogel *et al.*, "High gradients at SRF photoinjector cavities with low RRR copper cathode plug screwed to the cavity back wall", Oct. 2023. doi:10.48550/arXiv.2310.02974

[5] COMSOL AB, "COMSOL Multiphysics® simulation software", 2025. https://www.comsol.com

[6] D. Bazyl, K. Floettmann, E. Vogel, and I. Zagorodnov, "Multiphysics analysis of cryogenically cooled photocathode in a continuous wave SRF injector cavity", *Phys. Rev. Accel. Beams*, vol. 29, no. 1, p. 013402, Jan. 2026. doi:10.1103/9jyv-hfxy

[7] N. J. Simon, E. S. Drexler, and R. P. Reed, *Properties of Copper and Copper Alloys at Cryogenic Temperatures*. Gaithersburg, MD: National Institute of Standards and Technology, 1992.

[8] T. Schilcher, "Wärmeleitvermögen von Niob bei kryogenischen Temperaturen", Diplomarbeit, Universität Regensburg, DESY, 1995.

[9] R. C. Dhuley, M. I. Geelhoed, and J. C. T. Thangaraj, "Thermal resistance of pressed contacts of aluminum and niobium at liquid helium temperatures", *Cryogenics*, vol. 93, pp. 86–93, 2018. doi:10.1016/j.cryogenics.2018.06.003

[10] E. T. Swartz and R. O. Pohl, "Thermal boundary resistance", *Rev. Mod. Phys.*, vol. 61, no. 3, pp. 605–668, 1989. doi:10.1103/RevModPhys.61.605